

Received March 7, 2018, accepted March 29, 2018, date of publication April 3, 2018, date of current version June 29, 2018.

Digital Object Identifier 10.1109/ACCESS.2018.2822720

# Compact Sequential Feeding Network With Quadruple Output Ports and Its Application for Wideband Circularly Polarized Antenna

MEIJUN QU<sup>1</sup>, LI DENG<sup>1</sup>, MINGXING LI<sup>2</sup>, LIDAN YAO<sup>2</sup>,  
AND SHUFANG LI<sup>1</sup>, (Senior Member, IEEE)

<sup>1</sup>School of Information and Communication Engineering, Beijing University of Posts and Telecommunications, Beijing 100876, China

<sup>2</sup>School of Electronic Engineering, Beijing University of Posts and Telecommunications, Beijing 100876, China

Corresponding author: Li Deng (dengl@bupt.edu.cn)

This work was supported in part by the National Natural Science Foundation of China under Grant 61427801 and Grant 61601040 and in part by the BUPT Excellent Ph.D. Students Foundation under Grant CX2017208.

**ABSTRACT** A compact single-layer series-type feeding network is proposed by utilizing two dual-band frequency-independent couplers in this paper. The overall size of the feeding network is further reduced by meandering the transmission lines. The proposed feeding network is quite suitable in the design of wideband circularly polarized antenna due to its wideband performance, identical amplitude and flat 90° successive shifts between two arbitrary adjacent ports. Based this, a wideband circularly polarized antenna for satellite application (L band and S band) is presented, fabricated, and measured employing the proposed feeding network. Four feeding strips are introduced to enhance the axial ratio (AR) bandwidth of the proposed antenna. The simulated AR bandwidth extends from 14.7% to 34.5% by loading the four feeding strips. The measured results indicate that the proposed antenna has numerous advantages, such as low-cost, low-profile (0.07λ<sub>0</sub>), wideband, high gain, wide AR bandwidth, and excellent circularly polarized feature. Note that the measurements agree reasonably well with the simulations.

**INDEX TERMS** Circularly-polarized antenna, compact, high-gain, series-type feeding network, wideband, wide AR bandwidth.

## I. INTRODUCTION

Many countries are building and upgrading their satellite positioning systems in recent years such as Global Positioning System (GPS) of the United States of America, Beidou-2 (BD2) of China, Global Navigation Satellite System (GLONASS) of Russia, and Galileo Positioning System (GALILEO) of Europe. Due to the massive growth of the spacecraft systems, satellite communications, navigation and positioning systems [1]–[9], broadband microstrip circularly-polarized (CP) antenna with wide half-power beamwidth draws a lot of attention. CP antenna could reduce multipath fading and “Faraday rotation” effect. In addition, wideband performance of the CP antenna could be compatible with different satellite systems. It is known that a CP antenna with improved low elevation could receive more useful signals. Hence, wide half-power beamwidth (HPBW) of the CP antenna is needed to maximize the coverage of the satellites and is required for precise real-time position applications [4], [10], [11]. By inserting a parasitic ring, the vertical HPBW of the antenna could be wider and the gain for low elevation angle is improved [4]. In [10], both

AR and power beamwidth of CP radiation are widened when the CP antenna composed of two appropriate type of paired folded dipoles. In [11], the  $|E_{\theta}|$  and  $|E_{\varphi}|$  radiation patterns can be made nearly equalized over a large angular range, if the spacing  $L$  between two parallel slots in the antenna is selected as  $0.45 \lambda_0$ . Nevertheless, high gain characteristic of the antenna and HPBW are mutually restricted. Therefore, the proposed antenna is required to increase HPBW as much as possible while maintaining high gain feature.

The quadrifilar helix antenna (QHA) is suitable for satellite communication due to its excellent axial ratio and cardioid-shaped radiation pattern [2], [7], and [12]. However, as a kind of resonant antenna, the volume of the QHA is quite large. Thus, it is not suitable in the miniaturization and integration of RF front-end systems. Low-profile property becomes another design challenge, except the inherent narrow impedance and axial ratio bandwidth of the microstrip CP antenna.

Nowadays, sequential rotation technique [12]–[20] is applied to feed CP antennas like quadrifilar helical antennas [12]–[14] or antenna arrays [15]–[18]. Excellent CP

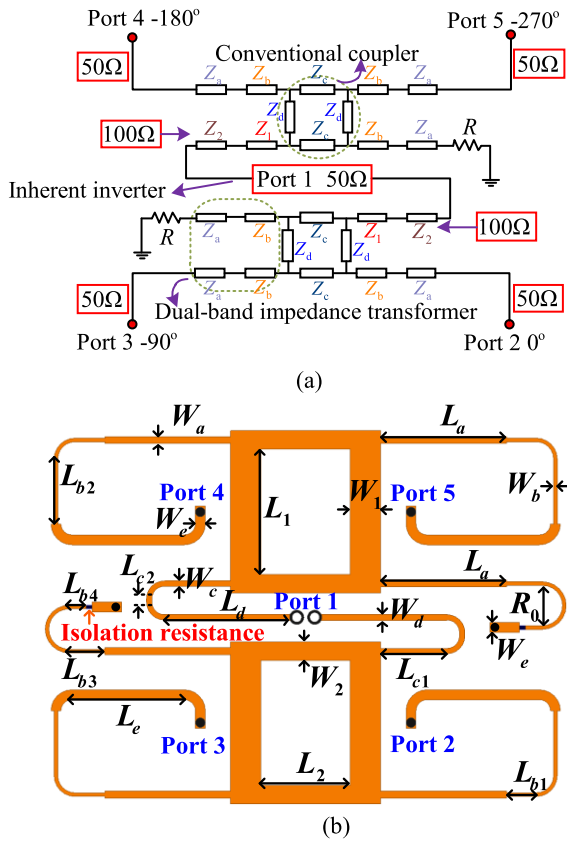


FIGURE 1. (a) The equivalent circuit and (b) layout of the proposed CSFN with geometrical parameters.

characteristics and low voltage standing-wave ratio over a wide frequency band of the CP antenna could be achieved by loading the series-type feeding network. The outputs of the feeding networks could provide signals with equal amplitude and successive 90° phase differences between two adjacent ports. In [19], the feeding network consists of an out-of-phase power divider and two Wilkinson power dividers with two 90° phase shifters. An out-of-phase power divider and two couplers are combined to form a broadband feeding network [12], [15]. The out-of-phase power divider is designed by inserting a conductor plate into the mid-layer of a double-sided parallel stripline. Therefore, two-layer substrate is needed during the processing of the feeding network, which is not conducive to miniaturization and low cost. Those aforementioned feeding networks are large or complex for practical applications.

This paper proposes a novel compact single-layer wideband sequential feeding network utilizing two meandering dual-band frequency-independent couplers. Afterwards, a wideband CP antenna for satellite application is designed based on the proposed feeding network. From the measured results, it is demonstrated that due to the introduction of the feeding network, the 10-dB impedance bandwidth and AR bandwidth of the proposed antenna could be enhanced. To further improve the AR

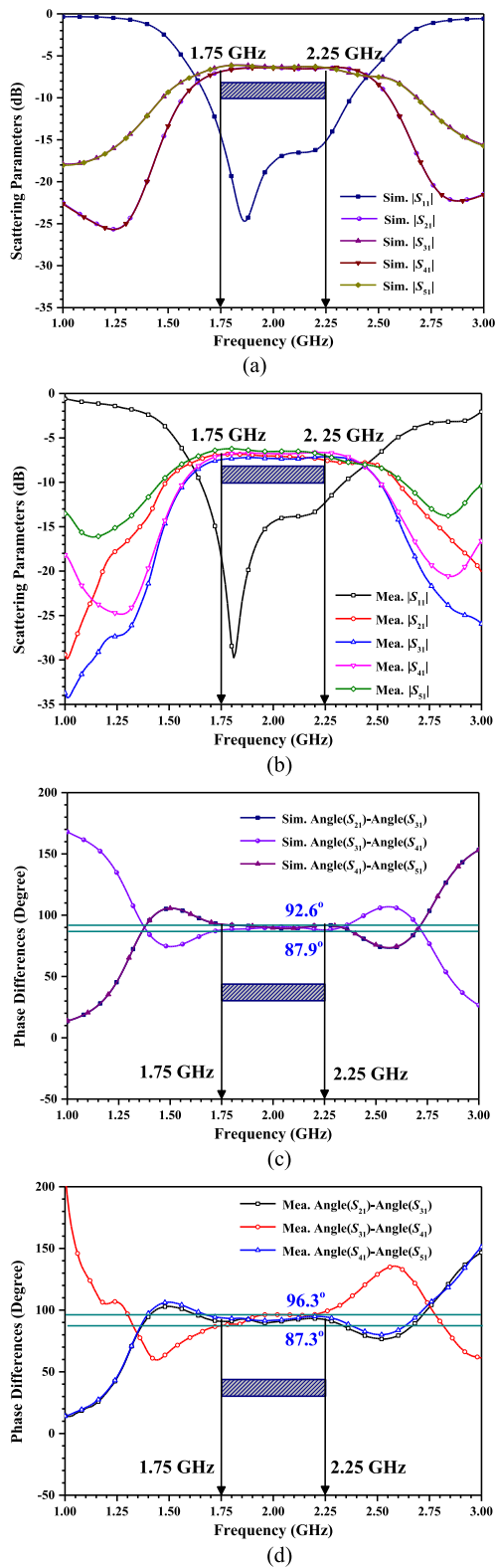
TABLE 1. The geometrical parameters of the proposed antenna.

Parameters	Values	Parameters	Values
$W$	130 mm	$L$	130 mm
$W_1$	5.1 mm	$L_1$	21 mm
$W_2$	3.12 mm	$L_2$	15 mm
$W_a$	1.15 mm	$L_a$	21.1 mm
$W_b$	0.61 mm	$L_{b1}$	5 mm
$L_{b2}$	10.9 mm	$L_{b3}$	6 mm
$L_{b4}$	2.8 mm	$W_c$	0.9 mm
$L_{c1}$	11 mm	$L_{c2}$	0.57 mm
$W_d$	1.05 mm	$L_d$	21.4 mm
$W_e$	1.66 mm	$L_e$	18.9 mm
$R_0$	3.4 mm	$H_1$	0.762 mm
$H_2$	9 mm	$R_1$	32.7 mm
$R_2$	24 mm	$d_1$	8 mm
$d_2$	2 mm	$S$	2 mm
$\theta$	60°		

bandwidth, four feeding strips are utilized to excite the circular ring patch. To sum up, the proposed antenna has a number of advantages including low-cost, low-profile, wideband, high gain, wide AR bandwidth and excellent CP feature. Thus, it is quite suitable for satellite application.

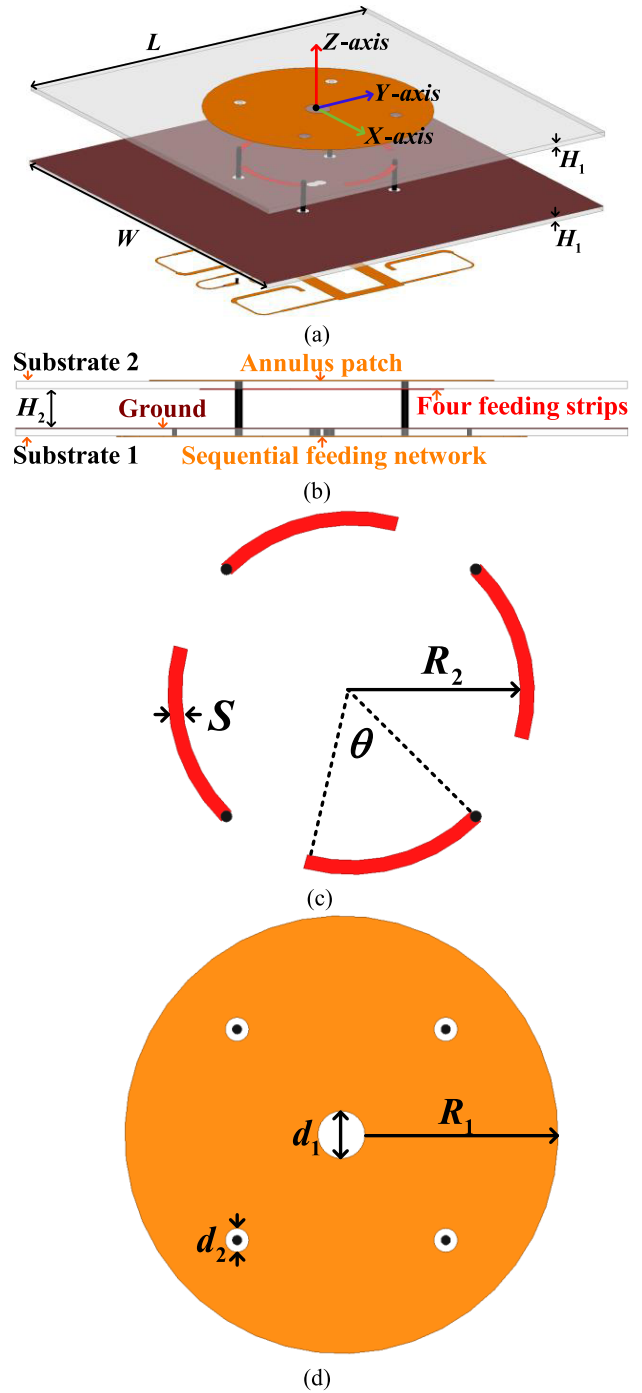
## II. COMPACT SEQUENTIAL FEEDING NETWORK DESIGN

Fig. 1(a) displays the equivalent circuit of the proposed compact sequential feeding network (CSFN). The CSFN consists of two dual-band frequency-independent branch-line couplers [20], which is excited by a coaxial cable. The employed dual-band coupler with 12-section transmission lines is composed of a conventional branch-line coupler and four two-section impedance transformers. The inherent four-section branch lines with impedance values of  $Z_c$  and  $Z_d$  are utilized to form a conventional branch-line coupler. While the impedance transformers are two independent two-section dual-band impedance transformers that can realize impedance transformation from source impedance to load impedance at both two frequencies  $f_1$  and  $f_2$ . By decreasing the distance between the two resonant frequencies, the feeding network could achieve wideband performance. Note that the 12-section transmission lines are with the same electrical length ( $\theta = 90^\circ$ ).  $R$  is the isolation resistance with 50  $\Omega$ , which is installed to make the isolation port of coupler connect to the ground. The inner and outer conductors of the coaxial cable are welded to the two input ports of the dual-band couplers, respectively. Therefore, two-way signals with equal amplitude and 180° phase differences could be loaded to the two couplers. In addition, the input impedances of the two applied couplers should be  $50 \times 2 = 100 \Omega$  due to the parallel relation of the two couplers. The four output load impedances of the proposed CSFN are set as 50  $\Omega$ , which can directly connect with other standard RF devices. The corresponding layout of the CSFN is illustrated in Fig. 1(b) marked with the



**FIGURE 2.** (a) Simulated and (b) measured scattering parameters, (c) simulated and (d) measured phase information of the proposed CSFN.

geometrical parameters. The proposed CSFN is constructed on the substrate of Rogers RO4350B substrates with a dielectric constant of 3.66, a loss tangent of 0.004, and thickness



**FIGURE 3.** Configuration of the proposed wideband CP antenna based on the CSFN. (a) Three-dimensional view, (b) side view, top view of the (c) four feeding strips and (d) annulus patch.

of 0.762 mm. It can be found that the transmission lines of the couplers are bent to further reduce the total size of the proposed CSFN. The geometrical parameters of the final CSFN are listed in TABLE I.

The simulated and measured scattering parameters and phase information of the proposed CSFN are presented in Figs. 2(a-d). From the Fig. 2(a), the simulated 10-dB

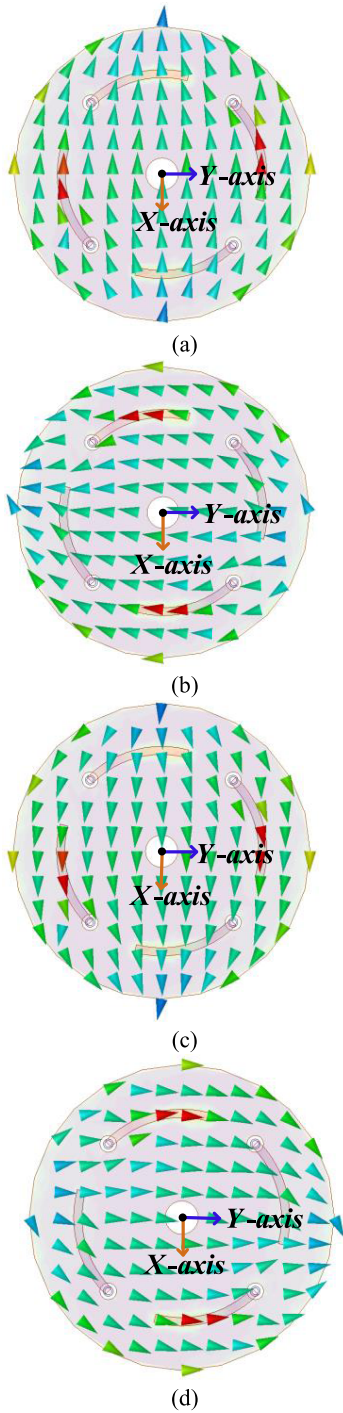
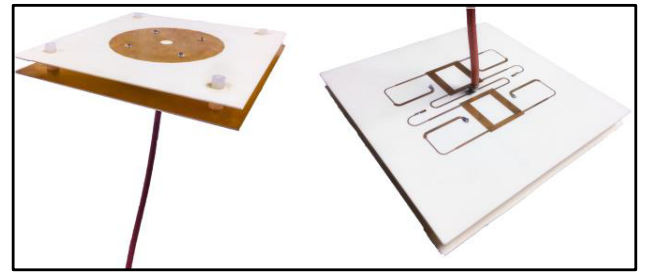
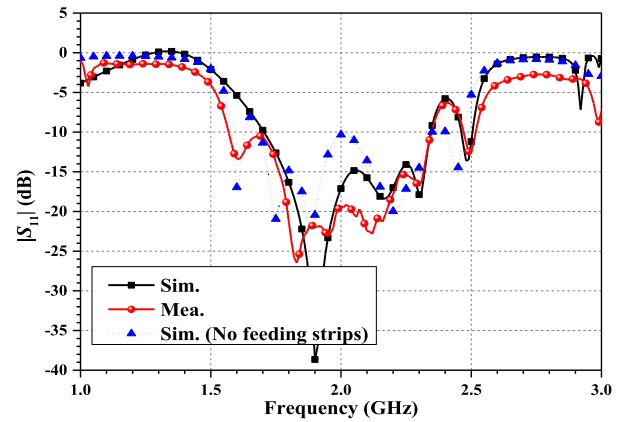


FIGURE 4. Current distributions of the annulus patch with phases of (a) 0°, (b) 90°, (c) 180°, and (d) 270°, respectively.

impedance bandwidth of the proposed CSFN is about 34% from 1.68 to 2.37 GHz, while the measured 10-dB impedance bandwidth is 34.6% from 1.65 to 2.34 GHz from Fig. 2(b). The simulated and measured insertion losses are  $-6.5 \pm 0.38$  dB and  $-6.5 \pm 1$  dB within the frequency range of 1.75 to 2.25 GHz, respectively. A measured 90° phase shift with the largest deviation of almost  $\pm 2.6^\circ$  comparing with the



(a)



(b)

FIGURE 5. (a) The photograph of the proposed wideband CP antenna loaded with CSFN, (b) the simulated and measured reflection coefficients of the proposed antenna.

simulated ones of  $\pm 6.3^\circ$  can be observed from Figs. 2(c-d). Based on this, a wideband CSFN with flat phase difference between two adjacent ports could be achieved since the  $f_1$  and  $f_2$  are selected closely in this case. The sequential rotation feeding technique of the proposed CSFN has a great potential in improving operating bandwidth and CP characteristics of the microstrip antennas. Hence, a wideband CP antenna is designed adopting the proposed CSFN for demonstration in the following section.

### III. WIDEBAND CIRCULARLY-POLARIZED ANTENNA WITH THE PROPOSED FEEDING NETWORK DESIGN

Figs. 3(a-d) present the configuration and structural details of the proposed wideband CP antenna based on CSFN. The antenna is designed on a two-layer printed circuit board connected by the four copper columns. The bottom layer is the proposed CSFN, while the top layer is the radiator constructed on the same substrate. The ground of the proposed CSFN is on the upper surface since the radiation performance of the couplers could affect that of the CP antenna. Note that the ground is the common ground for the proposed CSFN and the radiator. The upper layer consists of four feeding strips and an annulus patch. Four output ports (Ports 2-5) of the CSFN are connected to the four feeding strips by the copper column. It can be observed that there are four circular slots etched on the ground which could avoid short circuit. In addition, four circular slots are existed in the



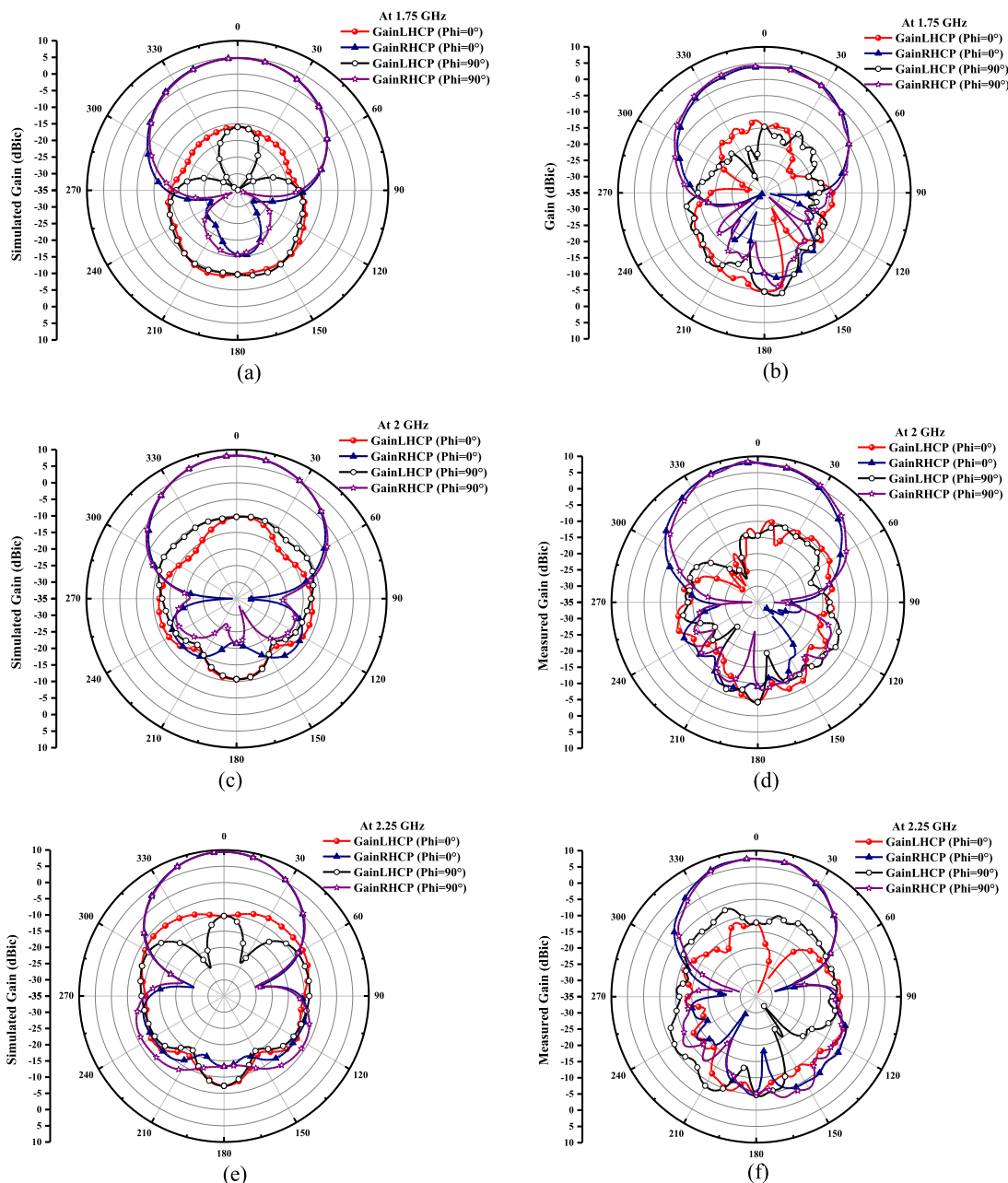


**FIGURE 6.** (a) Simulated and (b) measured 2-D radiation patterns of the proposed wideband CP antenna based on CSFN in XOZ and YOZ planes at 1.75 GHz. (c) Simulated and (d) measured 2-D radiation patterns of the proposed wideband CP antenna based on CSFN in XOZ and YOZ planes at 2 GHz. (e) Simulated and (f) measured 2-D radiation patterns of the proposed wideband CP antenna based on CSFN in XOZ and YOZ planes at 2.25 GHz.

annulus patch as well at the four feeding ports. The four copper columns can be installed and welded conveniently by this way. The final optimized geometry parameters are tabulated in TABLE I. The proposed CSFN and antenna are simulated with the full-wave simulation tool, Ansoft HFSS.

In the existing literature, several kinds of coupled patches are used for improving the bandwidth of CP antenna [1], [3], [21]–[24]. Nevertheless, these antennas need a thick substrate or air-layer between the parasitic patch and driven patch to enhance the performance. The feeding strips

and annulus patch of the proposed antenna are printed directly on a single substrate. Therefore, compact size and low profile could be achieved. The utilization of the four feeding strips is also the key to make the proposed antenna obtain excellent AR bandwidth. To further explain this reason, an antenna without feeding strips is simulated as well. From the Fig. 5(b), the simulated 10-dB return loss bandwidth is close to that of the antenna with feeding strips even though the impedance matching is slightly worse. The simulated AR curves are exhibited in Fig. 7(b). It can be seen that the bandwidth of AR

below 3 dB is 14.7% from 2.02 to 2.34 GHz without feeding strips. The simulated AR bandwidth would be enhanced significantly to 34.5% from 1.63 to 2.31 GHz if the four feeding strips are loaded.

The proposed CSFN is connected to the four feeding strips to excite the annulus patch, which makes the proposed antenna achieve excellent right-hand CP function. This is because the proposed CSFN could provide four-way energy with identical amplitude and 90° phase shifts between two arbitrary adjacent ports. To prove that, current distributions of the annulus patch at 2 GHz with phase of 0°, 90°, 180°, and 270° are depicted in Fig. 4. It can be found that the direction of the current with the phase of 0° is along with -X-axis. The current direction is consistent with -Y-axis when the phase is changed to 90°. While the direction currents points to X-axis and Y-axis, corresponding to the phases of 180° and 270°. Namely, the current rotates counterclockwise on the annulus patch during one cycle. Therefore, the RHCP characteristic of proposed antenna could be achieved.

A wideband CP example is fabricated and measured for verification. The photograph of the prototype is shown in Fig. 5(a). The scattering parameters of the proposed antenna are measured by Vector Network Analyzer (Agilent E5071C). While the far-field radiation performances are measured by the SATIMO measurement system in a microwave anechoic chamber. As depicted in Fig. 5(b), the simulated 10-dB impedance bandwidth is 31.1% from 1.71 to 2.34 GHz. The measured bandwidth of return loss above 10 dB is 39.4% from 1.57 to 2.34 GHz as predicted in the simulation. Hence, the wideband function of the proposed CSFN-based antenna could be achieved. Figs. 6(a-f) plot the simulated and measured 2-D radiation patterns in *XOZ* and *YOZ* planes at 1.75 GHz, 2 GHz and 2.25 GHz, respectively. It can be seen that the proposed antenna has directional radiation pattern, and the RHCP is the co-polarization. It is shown that the RHCP are much larger than the left-hand circular polarization (LHCP), denoting that excellent RHCP function of the proposed antenna could be obtained. The simulated boresight gain at 1.75 GHz, 2 GHz and 2.25 GHz is 4.79 dBic, 8.17 dBic and 9.42 dBic, respectively. While the measured ones are 3.88 dBic, 8 dBic and 7.59 dBic at 1.75 GHz, 2 GHz and 2.25 GHz, respectively. It can be concluded that the proposed antenna can provide stable symmetrical directional radiation patterns with high gain through the whole operating band.

The measured boresight gain response is compared with the simulated result in Fig. 7(a). The maximum measured gain is 9.27 dBic at 2.11 GHz, and the gain above 6 dBic is from 1.9-2.34 GHz. The measured gain decreases out of the operating frequency bands. For example, the gain is attenuated to -12.2 dBic at 1.45 GHz and -11.54 dBic at 2.75 GHz. In addition, the proposed antenna achieves about 84% maximum total radiation efficiency near the 2.1 GHz. The simulated and measured AR bandwidths of the proposed antenna are displayed in Fig. 7(b). The measured AR band-

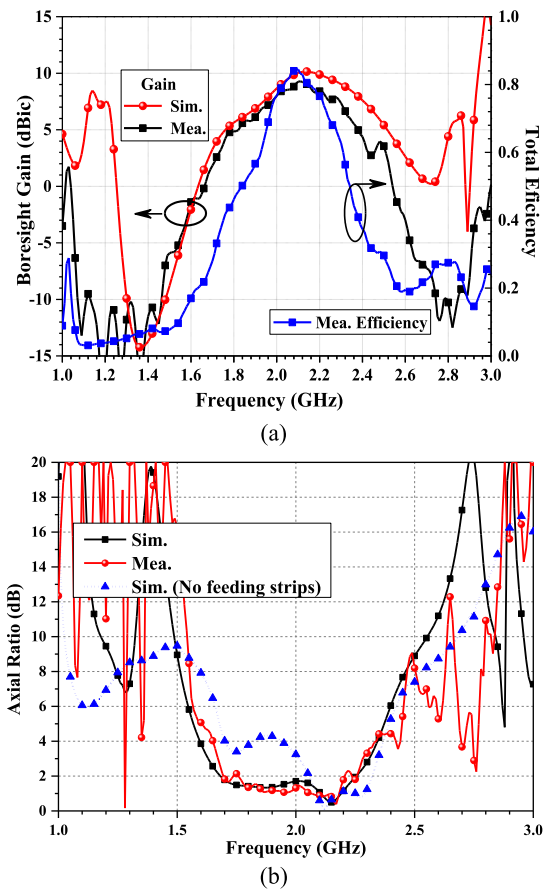


**FIGURE 7. Simulated and measured (a) gain responses and measured total efficiency, (b) axial ratios of the proposed wideband CP antenna based on CSFN.**

width below 3 dB is 30.9% from 1.67 to 2.28 GHz, comparing with the simulated one 34.5% from 1.63 to 2.31 GHz. Thus, a high-gain CP antenna with wide AR bandwidth is finally achieved.

Excellent agreement between the simulated and measured results is observed, demonstrating the validity of our proposed antenna design. Note that the discrepancies between the simulated and measured results are created due to connector losses, the effects of soldering, and errors in fabrication. To sum up, all the simulated and measured results clearly indicate that the proposed antenna achieves a good performance in terms of impedance bandwidth, radiation pattern, gain and AR bandwidth. Therefore, the proposed antenna is an excellent candidate for satellite communication. It should be mentioned that if the RF front-ended system is differential, the proposed antenna based on the feeding network could be connected with the RF front-ended system by adopting two coaxial cables terminated by SMA connectors [25]–[27]. Balanced feeding could be achieved by this method.

In order to highlight the advantages of the proposed wideband antenna, the measured performance comparison between the proposed antenna and other designs in the

TABLE 2. The Performance Comparison of CP Antennas.

Refs	Impedance bandwidth	3-dB AR bandwidth	Axial Height
[9]	11.4% (1.217 to 1.364 GHz)	2.1% (1.252 to 1.289 GHz)	0.18 $\lambda_0$
	8.4% (1.505 to 1.637 GHz)	2.2% (1.534 to 1.572 GHz)	( $\lambda_0 = 1.268$ GHz)
[12]	49.2% (0.98 to 1.62 GHz)	21.9% (1.1 to 1.37 GHz)	0.4 $\lambda_0$
		3.2% (1.53 to 1.58 GHz)	( $\lambda_0 = 1.22$ GHz)
[13]	1.1 to 1.27 GHz (RL >10 dB)	★	0.34 $\lambda_0$
	1.54 to 1.7 GHz (RL >10 dB)		( $\lambda_0 = 1.2276$ GHz)
[28]	VSWR < 2:	28.3% (3.62 to 4.75 GHz)	0.07 $\lambda_0$
	36% (3.32 to 4.76 GHz)		( $\lambda_0 = 4$ GHz)
[29]	VSWR < 2:	33.2% (5.20–7.19 GHz)	0.19 $\lambda_0$
	36.2% (5.04–7.21 GHz)		( $\lambda_0 = 6$ GHz)
[30]	VSWR < 2:	23.33% (5.65–7.05 GHz)	0.19 $\lambda_0$
	36.67% (5.16–7.36 GHz)		( $\lambda_0 = 6$ GHz)
[31]	51% (3.28–5.54 GHz).	27% (3.5–4.6 GHz)	0.12 $\lambda_0$
			( $\lambda_0 = 4.25$ GHz)
<b>This work</b>	<b>39.4% (1.57 to 2.34 GHz)</b>	<b>30.9% (1.67 to 2.28 GHz)</b>	<b>0.07<math>\lambda_0</math></b> ( $\lambda_0 = 2$ GHz)

★: No available data.

previous literatures [9], [12]–[13], [28]–[31] is provided in TABLE II.

IV. CONCLUSION

A single-layer feeding network is proposed in this paper which performs a four-way power dividing with identical amplitude and sequentially rotated phase shifting. The series-type feeding network has a number of advantages including compact size, wideband, same amplitude and flat phase difference between the two arbitrary output ports. To verify the effectiveness and practicality of the feeding network, a wideband RHCP antenna for satellite application (L band and S band) based on the CSFN is designed, fabricated and measured. The measured results exhibit that the 10-dB impedance bandwidth is about 39.4% over 1.57 to 2.34 GHz. The AR bandwidth is -30.9% from 1.67 to 2.28 GHz. Such a wide AR bandwidth benefits from the introduction of the four feeding strips. Moreover, the gain is above 6 dBic from 1.9 to 2.34 GHz. In summary, the proposed antenna design exhibits low-profile, wideband, excellent CP characteristic, wideband AR bandwidth and high-gain properties.

ACKNOWLEDGMENT

Meijun Qu conceived the idea and was responsible for the full-wave simulations and the physical-structures construction of the antenna model. Li Deng, Lidan Yao and Shufang Li provided various constructive comments and suggestions for improving this work.

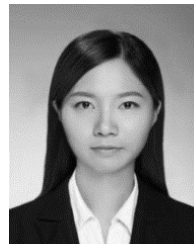
REFERENCES

- [1] D. M. Pozar and S. M. Duffy, "A dual-band circularly polarized aperture-coupled stacked microstrip antenna for global positioning satellite," *IEEE Trans. Antennas Propag.*, vol. 45, no. 11, pp. 1618–1625, Nov. 1997.
- [2] Q.-X. Chu, W. Lin, W.-X. Lin, and Z.-K. Pan, "Assembled dual-band broadband quadrifilar helix antennas with compact power divider networks for CNSS application," *IEEE Trans. Antennas Propag.*, vol. 61, no. 2, pp. 516–523, Feb. 2013.
- [3] Q. Liu, Y. Liu, Y. Wu, M. Su, and J. Shen, "Compact wideband circularly polarized patch antenna for CNSS applications," *IEEE Antennas Wireless Propag. Lett.*, vol. 12, pp. 1280–1283, 2013.
- [4] Z.-K. Pan, W.-X. Lin, and Q.-X. Chu, "Compact wide-beam circularly-polarized microstrip antenna with a parasitic ring for CNSS application," *IEEE Trans. Antennas Propag.*, vol. 62, no. 5, pp. 2847–2850, May 2014.
- [5] E. Ghafari and D. N. Aloï, "Single-pin, single-layer, dual-band patch antenna for global positioning system and satellite digital audio radio system automotive applications," *IET Microw., Antennas Propag.*, vol. 8, no. 13, pp. 1066–1074, Oct. 2014.
- [6] N. Kushwaha and R. Kumar, "Compact coplanar waveguide-fed wideband circular polarised antenna for navigation and wireless applications," *IET Microw., Antennas Propag.*, vol. 9, no. 14, pp. 1533–1539, 2015.
- [7] Y.-H. Yang, J.-L. Guo, B.-H. Sun, and Y.-H. Huang, "Dual-band slot helix antenna for global positioning satellite applications," *IEEE Trans. Antennas Propag.*, vol. 64, no. 12, pp. 5146–5152, Dec. 2016.
- [8] C. Sun, Z. Wu, and B. Bai, "A novel compact wideband patch antenna for GNSS application," *IEEE Trans. Antennas Propag.*, vol. 65, no. 12, pp. 7334–7339, Dec. 2017.
- [9] X.-C. Wang, L. Sun, X.-L. Lu, S. Liang, and W.-Z. Lu, "Single-feed dual-band circularly polarized dielectric resonator antenna for CNSS applications," *IEEE Trans. Antennas Propag.*, vol. 65, no. 8, pp. 4283–4287, Aug. 2017.
- [10] Y. Luo, Q.-X. Chu, and L. Zhu, "A miniaturized wide-beamwidth circularly polarized planar antenna via two pairs of folded dipoles in a square contour," *IEEE Trans. Antennas Propag.*, vol. 63, no. 8, pp. 3753–3759, Aug. 2015.
- [11] N.-W. Liu, L. Zhu, and W.-W. Choi, "Low-profile wide-beamwidth circularly-polarised patch antenna on a suspended substrate," *IET Microw., Antennas Propag.*, vol. 10, no. 8, pp. 885–890, Mar. 2016.
- [12] Y. Wu, M. Qu, W. Wang, and Y. Liu, "A frequency-independent dual-band printed quadrifilar helix antenna using nonuniform, unequal-length, asymmetrical coupled lines," *Microw. Opt. Technol. Lett.*, vol. 58, no. 7, pp. 1728–1733, Apr. 2016.
- [13] G. Byun, H. Choo, and S. Kim, "Design of a dual-band quadrifilar helix antenna using stepped-width arms," *IEEE Trans. Antennas Propag.*, vol. 63, no. 4, pp. 1858–1862, Apr. 2015.
- [14] Z.-Y. Zhang, L. Yang, S. L. Zuo, M. U. Rehman, G. Fu, and C. Zhou, "Printed quadrifilar helix antenna with enhanced bandwidth," *IET Microw. Antennas Propag.*, vol. 11, no. 5, pp. 732–736, 2017.
- [15] Q. Liu, J. Shen, H. Liu, Y. Wu, M. Su, and Y. Liu, "Low-cost compact circularly polarized directional antenna for universal UHF RFID handheld reader applications," *IEEE Antennas Wireless Propag. Lett.*, vol. 14, no. , pp. 1326–1329, 2015.
- [16] A. B. Smolders and U. Johannsen, "Axial ratio enhancement for circularly-polarized millimeter-wave phased-arrays using a sequential rotation technique," *IEEE Trans. Antennas Propag.*, vol. 59, no. 9, pp. 3465–3469, Sep. 2011.
- [17] A. Chen, Y. Zhang, Z. Chen, and C. Yang, "Development of a Ka-band wideband circularly polarized 64-element microstrip antenna array with double application of the sequential rotation feeding technique," *IEEE Antennas Wireless Propag. Lett.*, vol. 10, pp. 1270–1273, 2011.
- [18] A. B. Smolders and H. J. Visser, "Low side-lobe circularly-polarized phased arrays using a random sequential rotation technique," *IEEE Trans. Antennas Propag.*, vol. 62, no. 12, pp. 6476–6481, Dec. 2014.
- [19] X.-Q. Yang, Z.-H. Yan, P. Xu, T.-L. Zhang, Z. Zhu, and T. Liang, "A broadband printed quadrifilar helical antenna with a novel compact broadband feeding network," *Prog. Electromag. Res. C*, vol. 51, pp. 103–109, 2014.
- [20] Y. Wu, S. Y. Zheng, S. W. Leung, Y. Liu, and Q. Xue, "An analytical design method for a novel dual-band unequal coupler with four arbitrary terminated resistances," *IEEE Trans. Ind. Electron.*, vol. 61, no. 10, pp. 5509–5516, Oct. 2014.
- [21] Nasimuddin, K. P. Esselle, and A. K. Verma, "Wideband circularly polarized stacked microstrip antennas," *IEEE Antennas Wireless Propag. Lett.*, vol. 6, pp. 21–24, 2007.

- [22] Nasimuddin, K. P. Esselle, and A. K. Verma, "Wideband high-gain circularly polarized stacked microstrip antennas with an optimized c-type feed and a short horn," *IEEE Trans. Antennas Propag.*, vol. 56, no. 2, pp. 578–581, Feb. 2008.
- [23] H. Oraizi and R. Pazoki, "Radiation bandwidth enhancement of aperture stacked microstrip antennas," *IEEE Trans. Antennas Propag.*, vol. 59, no. 12, pp. 4445–4453, Dec. 2011.
- [24] A. Katyal and A. Basu, "Analysis and optimisation of broadband stacked microstrip antennas using transmission line model," *IET Microw., Antennas Propag.*, vol. 11, no. 1, pp. 81–91, Jan. 2017.
- [25] F. Sarrazin, S. Pflaum, and C. Delaveaud, "Radiation efficiency improvement of a balanced miniature IFA-inspired circular antenna," *IEEE Antennas Wireless Propag. Lett.*, vol. 16, pp. 1309–1312, 2017.
- [26] X. Qing, C. K. Goh, and Z. N. Chen, "Impedance characterization of RFID tag antennas and application in tag co-design," *IEEE Trans. Microw. Theory Techn.*, vol. 57, no. 5, pp. 1268–1274, May 2009.
- [27] H. Ge, Y. Yao, J. Yu, X. Chen, and D. Valderas, "Straight-forward impedance measurement for balanced RFID tag antenna," *Electron. Lett.*, vol. 52, no. 3, pp. 181–182, 2016.
- [28] Nasimuddin, Z. N. Chen, and X. Qing, "Bandwidth enhancement of a single-feed circularly polarized antenna using a metasurface: Metamaterial-based wideband CP rectangular microstrip antenna," *IEEE Antennas Propag. Mag.*, vol. 58, no. 2, pp. 39–46, Apr. 2016.
- [29] K. Agarwal, Nasimuddin, and A. Alphones, "Wideband circularly polarized AMC reflector backed aperture antenna," *IEEE Trans. Antennas Propag.*, vol. 61, no. 3, pp. 1456–1461, Mar. 2013.
- [30] K. Agarwal, Nasimuddin, and A. Alphones, "Unidirectional wideband circularly polarised aperture antennas backed with artificial magnetic conductor reflectors," *IET Microw., Antennas Propag.*, vol. 7, no. 5, pp. 338–346, Apr. 2013.
- [31] Nasimuddin, Z. N. Chen, and K. P. Esselle, "Wideband circularly polarized microstrip antenna array using a new single feed network," *Microw. Opt. Technol. Lett.*, vol. 50, no. 7, pp. 1784–1789, 2008.



**MINGXING LI** received the B.S. degree from the College of Information Science and Technology, Henan University of Technology, Zhengzhou, China, in 2015. He is currently pursuing the Ph.D. degree with the Beijing University of Posts and Telecommunications (BUPT). In 2015, he started his research as a graduate at BUPT. His research interests include microwave passive components, RF, and radar systems.



**LIDAN YAO** was born in Hebei, China, in 1992. She received the B.Sc. degree in communication engineering from Yanshan University, Qinhuangdao, China, in 2014. She is currently pursuing the Ph.D. degree in electronic engineering with the Beijing University of Posts and Telecommunications, Beijing, China. Her research interests include differential microwave passive components design.



**MEIJUN QU** received the B.S. degree from the College of Physics and Electronics, Shanxi University, Taiyuan, China, in 2015. She is currently pursuing the Ph.D. degree with the School of Information and Communication Engineering, Beijing University of Posts and Telecommunications, Beijing, China. Her research interests include microwave passive component, antenna, metamaterial, and electromagnetic compatibility.



**LI DENG** was born in Sichuan, China, in 1982. He received the B.Eng. and M.Eng. degrees in communication engineering from Beijing Jiaotong University in 2004 and 2007, respectively, and the Ph.D. degree in communication engineering from the Beijing University of Posts and Telecommunications (BUPT), Beijing, China, in 2010. In 2012, he joined BUPT, where he is currently an Associate Professor with the School of Information and Communication Engineering.

His research interests include electromagnetic theory, metamaterial, and transformation optics.



**SHUFANG LI** (SM'09) received the Ph.D. degree from the Department of Electrical Engineering, Tsinghua University, Beijing, China, in 1997. She is currently the Director of the Ubiquitous Electromagnetic Environment Center of Education Ministry, China, and the Director of the Joint Laboratory of Beijing University of Posts and Telecommunications and the State Radio Monitoring Center, China. Her research interests include the theory and design technology of radio

frequency circuits in wireless communication, EMI/EMC, simulation technology and optimization for radiation interfere on high-speed digital circuit, and so on. She received the Young Scientists Reward sponsored by the International Union of Radio Science. She has published hundreds of papers interiorly and overseas, as well as several textbooks, translation works, and patents.

...